

# Neutrophil chemotaxis in linear and complex gradients of interleukin-8 formed in a microfabricated device

Noo Li Jeon<sup>1†</sup>, Harihara Baskaran<sup>1†</sup>, Stephan K. W. Dertinger<sup>2</sup>, George M. Whitesides<sup>2</sup>, Livingston Van De Water<sup>1,3</sup>, and Mehmet Toner<sup>1\*</sup>

Published online: 1 July 2002, doi:10.1038/nbt712

Although a wealth of knowledge about chemotaxis has accumulated in the past 40 years, these studies have been hampered by the inability of researchers to generate simple linear gradients instantaneously and to maintain them at steady state. Here we describe a device microfabricated by soft lithography and consisting of a network of microfluidic channels that can generate spatially and temporally controlled gradients of chemotactic factors. When human neutrophils are positioned within a microchannel, their migration in simple and complex interleukin-8 (IL-8) gradients can be tested. The cells exhibit strong directional migration toward increasing concentrations of IL-8 in linear gradients. Neutrophil migration halts abruptly when cells encounter a sudden drop in the chemoattractant concentration to zero ("cliff" gradient). When neutrophils are challenged with a gradual increase and decrease in chemoattractant ("hill" gradient), however, the cells traverse the crest of maximum concentration and migrate further before reversing direction. The technique described in this paper provides a robust method to investigate migratory cells under a variety of conditions not accessible to study by earlier techniques.

Chemotaxis is the process of directed migration by cells in gradients of soluble molecules termed chemoattractants. This process is fundamentally important in cancer metastasis<sup>1</sup>, embryogenesis<sup>2</sup>, and wound healing<sup>3</sup>. Chemoattractants and their receptors have been well characterized in recent years and are potential therapeutic targets for intervention in wound healing, cancer, and inflammation<sup>4–6</sup>.

Over the past 40 years, several approaches<sup>7</sup> have been developed to study chemotaxis, including Boyden chamber<sup>8</sup>, collagen or fibrin gel<sup>9</sup>, under agarose<sup>10</sup>, orientation<sup>11</sup>, capillary<sup>12</sup>, and Dunn chamber<sup>13</sup> assays. In most of these assays, the gradients generated typically are not linear and change with time and position; an exception is the Dunn's chamber assay, which offers an improved methodology with an initial stabilization period followed by a slowly decaying gradient. Despite the knowledge about chemotaxis gained using these methods, further studies require the ability to instantaneously generate linear and complex gradients and maintain them at steady state. Linear steady-state gradients would provide an excellent model system to study the mechanism of cell motility under well-defined conditions.

Microfabrication has great promise for creating and controlling microenvironments in which cell behavior can be observed in real time<sup>14,15</sup>. Soft lithography with polydimethyl siloxane (PDMS) is customarily used as a stamping technique to prepare surfaces that are in a quasi-two-dimensional array. It has been extended recently to include three-dimensional micromolding<sup>15</sup>, making it possible to generate stable soluble or surface-adsorbed gradients with a microfluidic system<sup>14</sup>.

We have used this technology to generate stable, soluble chemoattractant gradients. These gradients were produced by controlled diffusive mixing of species in solution that flow inside a network of microchannels under conditions of low Reynolds number. We adapted the above method to study neutrophil chemotaxis by generating soluble linear gradients of IL-8 (refs 16–19). Two important biological observations were made: first, a population of neutrophils in stable chemoattractant gradients migrated in a propagation pattern; and second, when confronted with heterogeneous gradients, neutrophils exhibited unexpected behaviors, suggesting a sophisticated cellular sensing mechanism.

## Results

**Microfluidic gradient generator.** The microfluidic gradient generator used in this study<sup>14</sup> (Fig. 1) is composed of a piece of PDMS (25 × 50 mm) with an embedded network of microchannels bonded to a glass coverslip. The microfluidic network within the PDMS consists of a gradient-generating portion (Fig. 1A) and an observation portion (Fig. 1B). The gradient-generating portion incorporates a branched network of microchannels (50 μm wide) immediately downstream of the chemoattractant inlets. This pyramidal branched array of microchannels serves to split, combine, and mix fluid streams as they flow through the network of microfluidic channels. Each resulting microchannel contains a different proportion of the chemoattractant, and these are recombined in the main channel (500 μm wide) such that the concentration gradient is perpendicular to the chemoattractant flow and the gradient is maintained throughout the length (several mil-

<sup>1</sup>Center for Engineering in Medicine and Surgical Services, Massachusetts General Hospital, Harvard Medical School, and Shriners Hospitals for Children, Boston, MA 02114. <sup>2</sup>Department of Chemistry and Chemical Biology, Harvard University, Cambridge, MA 02138. <sup>3</sup>Center for Cell Biology and Cancer Research, Albany Medical College, Albany, NY 12208. <sup>†</sup>These authors contributed equally to this work. \*Corresponding author (mtoner@sbi.org).

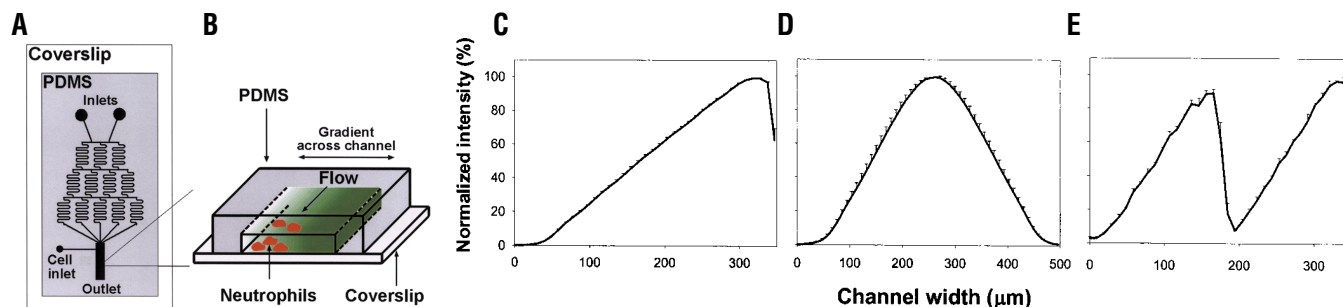


**Figure 1.** Schematic representations of the gradient generator and gradient characterization. (A) Top view of the whole device consisting of the gradient-generating and observation portions. (B) Three-dimensional schematic representation of the observation portion in which cells are exposed to gradients of chemoattractants. (C) Fluorescent tracer (FITC-dextran, relative molecular mass = 8 kDa) studies were carried out to characterize linear gradients generated across a channel width of 350  $\mu\text{m}$ . Fluorescent intensities were recorded at 5-min intervals from  $t = 0$  min to  $t = 60$  min after the establishment of the gradient. The intensities were normalized and time averaged and plotted as a function of channel width. (D) Similar results were obtained for hill (see text for details) gradient generated across a channel width of 500  $\mu\text{m}$ . (E) Similar results were obtained for cliff (see text for details) gradients generated across a channel width of 350  $\mu\text{m}$ .

limeters) of the main channel. The main channel serves as the observation portion in which the cells are placed. In most cases, the cells are placed at one side of the observation area using a separate inlet located next to the gradient-forming region. In some experiments, the cells are randomly seeded throughout the observation channel. For experiments in which a single, uninterrupted linear gradient of chemoattractant is tested (Fig. 1C), the device consists of dual inlets with Hank's balanced salt solution (HBSS) alone at one inlet and chemoattractant in HBSS at the other inlet<sup>14,15</sup>. For experiments in which either a cliff or hill gradient is needed, additional arrays of microchannel networks are used. By placing two linear gradient-generating networks in parallel along the migration path in a "head to head" configuration, we obtained a hill-type gradient (Fig. 1D), in which the IL-8 concentration increased linearly from 0 ng/ml to 50 ng/ml to a point midway in the channel, and then dropped linearly to 0 ng/ml. A related configuration, also involving parallel gradient-generating networks but this time in a "head to tail" arrangement, was used to obtain a cliff-type gradient, in which the IL-8 concentration increased linearly from 0 ng/ml to 50 ng/ml to a point midway in the channel, dropped precipitously to 0 ng/ml, and then increased linearly to 50 ng/ml (Fig. 1E). Figure 1C, D, and E shows experimental linear, hill, and cliff gradients in the device as monitored with fluorescent tracers. The average standard deviation of the gradients over a period of 60 min is about 7%, with no particular temporal trend, as determined by analysis of variance (ANOVA).

**Migration in stable linear gradients.** We chose neutrophils as model cells because they represent an important physiological system<sup>3,20</sup>. As a chemoattractant, we selected interleukin-8 (IL-8, 8 kDa), a heparin-binding polypeptide prominently expressed by lipopolysaccharide-stimulated human monocytes and belonging to the C-x-C family of chemokines<sup>21-23</sup>. We placed neutrophils inside the channels and followed their migration in uniform and linear gradients of IL-8 (Fig. 2). At the beginning of each experiment (Fig. 2, left panels), cells were

distributed either randomly (Fig. 2B, left) or deposited at the side of the migration chamber experiencing zero concentration of IL-8 (Fig. 2A, C, D, left). When IL-8 (50 ng/ml) was distributed uniformly throughout the chamber, the initial narrow band of cells broadened across the channel after 90 min (Fig. 2A, right as compared with left), serving as a control for chemokinesis. When cells were initially distributed evenly throughout the channel and a linear gradient of IL-8 (50  $\mu\text{g/ml}$  per 500  $\mu\text{m}$ ) was imposed, the neutrophils migrated toward the higher concentration of IL-8 (Fig. 2B). When cells were positioned at the lower IL-8 concentration side first and then subjected to a linear increase in IL-8 (0–50 ng/ml), the cells moved toward the higher IL-8 concentration (Fig. 2C). When the linear gradient was reversed so that the cells were attached initially in an environment of high IL-8 concentration, the initial band of cells spread out only slightly in the bottom half of the channel, indicating the net effect of random migration coupled with chemotaxis (Fig. 2D).

Next we assessed the normalized concentration of neutrophils as a function of channel length at time points 0, 10, 20, and 30 min, and under linear gradients 5, 50, and 500 ng/ml per 500  $\mu\text{m}$  (Fig. 3). We chose linear gradients to show the efficacy of the device in generating such gradients and also to simplify the solution of the mathematical model for chemotaxis to estimate biophysical parameters such as the chemotaxis coefficient. The specific gradients were selected based on a study by Foxman *et al.*<sup>24</sup>. The initial cell band moved in the direction of higher concentration of IL-8. Our results show that as the cells migrate through a gradient from 5 to 500 ng/ml per 500  $\mu\text{m}$ , the average migration speed also increases. Notably, the change in migration rate is more dramatic in the portion of the gradient between 5 and 50 ng/ml per 500  $\mu\text{m}$  than in the portion between 50 and 500 ng/ml per 500  $\mu\text{m}$ . The chemotaxis coefficient,  $\chi$ , is defined as the flux of neutrophils per unit gradient in the absence of random motility. Chemotaxis flux is the product of the chemotaxis coefficient and the chemoattractant concentration gradient, and is directly proportional to the number of cells migrating under chemotaxis. Values of  $\chi$  were calculated from the initial average speeds as a function of the chemoattractant gradients<sup>25</sup> (Table 1). The chemotaxis coefficient decreased with increasing chemoattractant gradient, a fairly common observation that suggests downregulation and saturation of receptor binding<sup>26</sup>. The chemotactic flux, on the other hand, increased as the gradient increased from 5 to 50 ng/ml per 500  $\mu\text{m}$  but did not change as the gradient increased further, suggesting saturation of the signals effecting neutrophil motility at IL-8 concentrations >50 ng/ml per 500  $\mu\text{m}$ .

**Migration in complex gradients.** Neutrophils migrating near an injury site are likely to be exposed to complex spatial patterns of chemoattractant. Using gradient-generating networks in parallel, we

**Table 1. Chemotaxis parameters of neutrophils**

Gradient	Chemotactic flux	Chemotaxis coefficient
$\frac{\partial I}{\partial x}$ (ng · ml <sup>-1</sup> · 500 $\mu\text{m}^{-1}$ )	$\chi \frac{\partial I}{\partial x}$ (10 <sup>5</sup> mm · s <sup>-1</sup> )	$\chi$ (10 <sup>7</sup> mm <sup>2</sup> · ml · ng <sup>-1</sup> · s <sup>-1</sup> )
5	1.2	12.0
50	5.5	5.8
500	6.0	0.6

Chemotactic flux is obtained by calculating the initial average speed of neutrophil density data at different homogeneous linear gradients (Fig. 3). Chemotaxis coefficients were obtained by dividing the chemotactic flux by the corresponding gradient<sup>25</sup>.

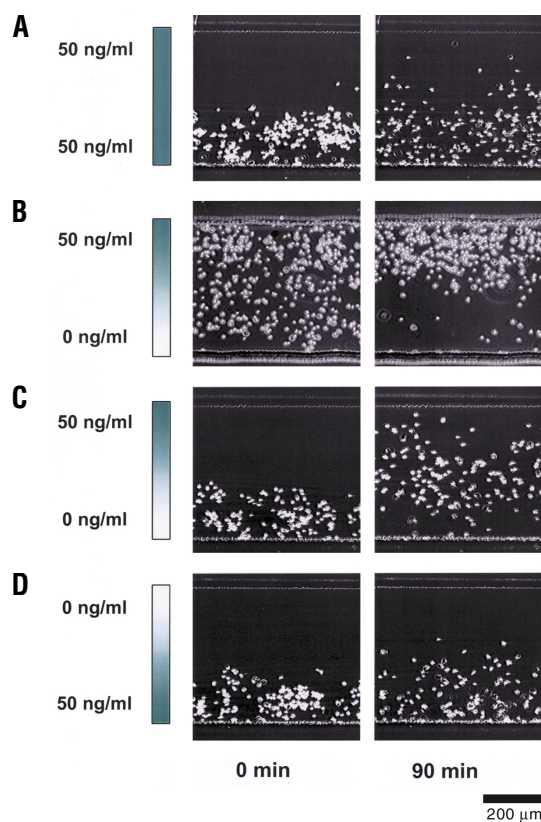


**Figure 2.** Neutrophil chemotaxis in homogeneous linear IL-8 gradients. Micrographs show cells at the beginning of each experiment (0 min; left panels), when they were distributed either randomly (B) or deposited at the bottom of the field of view (A, C, D), and at the conclusion of each experiment (90 min; right panels). (A) Random migration of neutrophils studied as a control in which IL-8 (50 ng/ml) was distributed uniformly across the channel. (B) Directed migration when cells were seeded evenly throughout the channel and a linear concentration gradient of 50 ng/ml per 500  $\mu\text{m}$  was applied. (C) Migration subjected to a linear increase in IL-8 (0–50 ng/ml). (D) Neutrophil migration when the linear gradient was reversed so that the cells were attached initially in an environment of high concentrations of IL-8 (D, left). Bar, 200  $\mu\text{m}$ .

obtained cliff- and hill-type gradients. When neutrophils were tested in a cliff gradient, many of the cells migrated up the gradient to a point coinciding with the edge of the cliff, but not farther (arrow in Fig. 4A). Analysis of individual cell tracks indicated that cells, when exposed to a sudden drop in concentration of IL-8, did not go over the locus of the maximum concentration (dashed line in Fig. 4B). Notably, a different behavior was observed when neutrophils encountered the hill gradient. This time the cells clustered in the middle of the channel (Fig. 4C). Furthermore, they were observed to migrate over the locus of the maximum concentration before turning around to move towards the maximum concentration of IL-8, indicating that they overshoot the maximum concentration and moved for some time after being exposed to a negative gradient (one of decreasing concentration; Fig. 4D). Figure 4E shows snapshots of a single neutrophil (arrow) that reversed direction after it overshoot the maximum concentration. The average time until cells ( $n = 6$ ) reversed direction was  $\sim 27.2 \pm 12.2$  min (mean  $\pm$  s.d.). Figure 4F shows migration speed of an individual cell as a function of channel width. Analysis of migratory speed data of individual cell tracks in hill experiments yielded an initial average speed of  $7.9 \pm 1.8$   $\mu\text{m}/\text{min}$  ( $n = 7$ ), which corresponds to a chemotaxis coefficient of  $6.6 \times 10^{-7}$   $\text{mm}^2 \text{ml} \text{s}^{-1} \text{ng}^{-1}$ . This is similar to the coefficient obtained from the results of migration in a homogeneous linear gradient of 50 ng/ml per 500  $\mu\text{m}$  (Table 1).

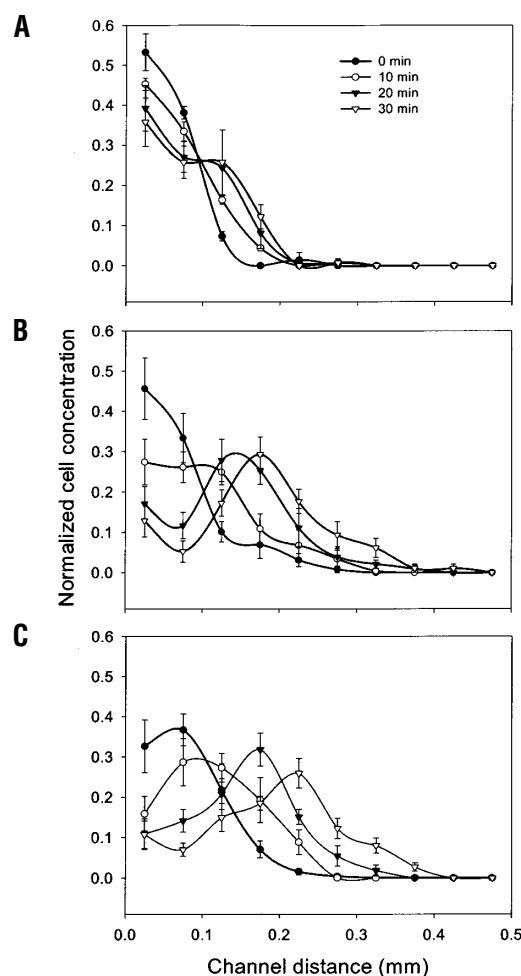


**Figure 3.** Quantification of neutrophil migration in homogeneous linear IL-8 gradients. At the beginning of each experiment, neutrophils were placed as a band along the side of the migration chamber that was exposed to zero IL-8 and a linear IL-8 concentration gradient was established in the chamber. Digital images of neutrophil migration were recorded at 20-s intervals and analyzed offline to obtain normalized cell concentration as a function of position and time. (A), (B), and (C) show neutrophil density data as a function of channel width at time points 0 ( $\bullet$ ), 10 ( $\circ$ ), 20 ( $\blacktriangledown$ ), and 30 ( $\nabla$ ) min under IL-8 gradients: 5 (number of independent experiments:  $n = 2$ ), 50 ( $n = 8$ ), and 500 ( $n = 6$ ) ng/ml per 500  $\mu\text{m}$ , respectively. Error bars show  $\pm$  s.d.

## Discussion

The chemotaxis device we describe can be used to generate stable gradients, manipulate the microenvironment of cells, and study the basic mechanisms of cell migration in real time. Its underlying principle is the use of low-Reynolds number flows to overcome diffusive forces and maintain the shape of the gradients in a microscale flow channel<sup>14</sup>. A key feature of the device is its ability to attain a steady state in which the concentration of chemoattractant at any position in the gradient is stable. This is accomplished by laminar flow, in which multiple streams of solutions containing different concentrations of chemoattractant flow side by side without turbulent mixing. Strict control of the composition of each of these streams is possible through an array of precisely defined branch points interspersed between a network of serpentine capillaries<sup>14</sup>. Despite the need for continuous flow through the system, the wall shear stress experienced by the cells is minimal ( $< 0.1$  dynes/ $\text{cm}^2$ ), well below the magnitude of shear forces ( $\geq 10$  dynes/ $\text{cm}^2$ ) experienced by endothelial cells in vessels.

One potential problem with our device is gradient smearing due to the diffusion of chemoattractant at the device surface<sup>27</sup> when streams

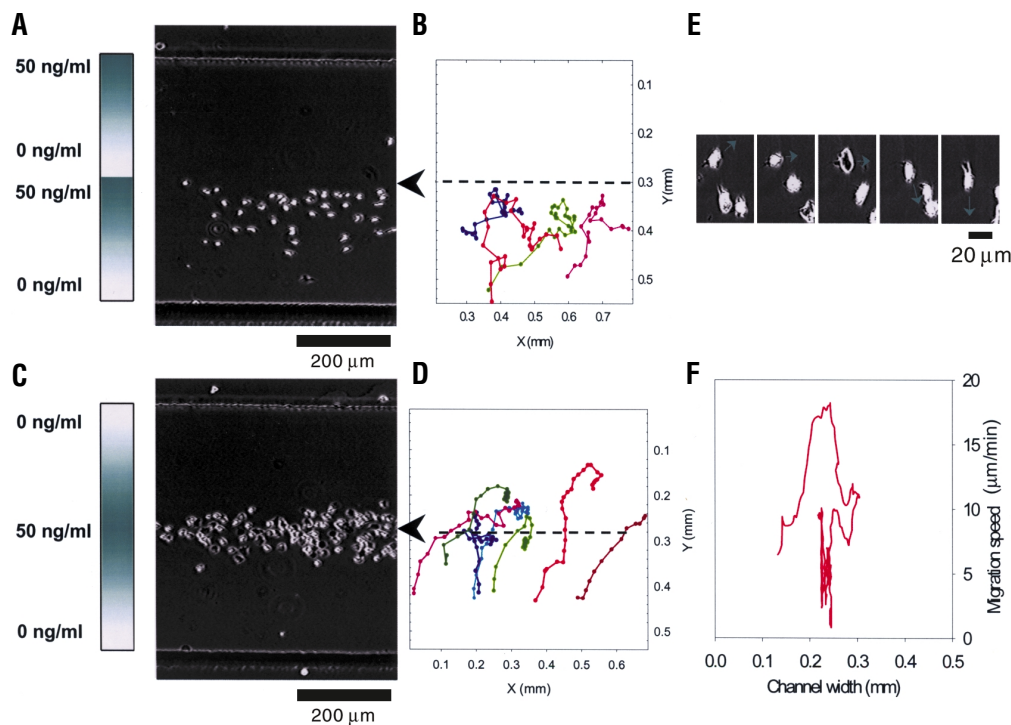


**Figure 4.** Neutrophil chemotaxis in heterogeneous linear IL-8 gradients. Cliff- and hill-type gradients were obtained by placing two linear gradient generators in parallel. At the beginning of each experiment, neutrophils were placed as a band along the side of the migration chamber that was exposed to zero IL-8. Digital images of neutrophil migration were obtained at 20-s intervals and recorded as cells were subjected to cliff- and hill-type gradients. (A) Neutrophils at the end (60 min) of exposure to cliff-type gradient. Bar, 200  $\mu\text{m}$ . (B) Tracks of cells exposed to cliff-type gradient. (C) Neutrophils at the end (60 min) of exposure to hill-type gradient. Bar, 200  $\mu\text{m}$ . (D) Tracks of cells exposed to hill-type gradient. (E) Snapshots of a single neutrophil (arrow) that reversed direction after it overshot a hill-type gradient. Bar, 20  $\mu\text{m}$ . (F) Migration speed of an individual cell in hill gradients as a function of channel width. Speeds were calculated from individual cell track data that were obtained every 20 s and filtered using Savitzky–Golay algorithm (Igor Pro, Wavemetrics, Lake Oswego, OR).

of different compositions are merged at the end. An expression that predicts the thickness of the diffusional band at the surface is<sup>27</sup>

$$\delta = (DH_z/U_a)^{1/3}$$

where  $\delta$  is the thickness of the diffusional band at the surface,  $D$  is the diffusion coefficient of IL-8 ( $2.5 \times 10^{-6} \text{ cm}^2/\text{s}$ ; ref. 28),  $H$  is the channel height (50  $\mu\text{m}$ ),  $z$  is the distance from the location of merging of individual streams (100  $\mu\text{m}$ ) and  $U_a$  is the average velocity (0.1 cm/s). The above expression predicts a diffusional band of 11  $\mu\text{m}$  thickness when two streams merge, and the net diffusional band thickness is  $\sim 10\%$  of the channel width. We consider this too small to have a major effect on the net concentration profile.

In conventional studies of neutrophil chemotaxis, the cells are placed at one location and the chemoattractant at another to start the experiment. The chemoattractant diffuses into the substrate as the cells migrate, resulting in time-variant concentration profiles and gradients of the chemoattractant. These conditions are not ideal for studying chemotaxis, as they typically yield only qualitative results; to describe the temporal and spatial variation of the chemoattractants quantitatively, mathematical models must be used extensively<sup>29</sup>. This qualitative approach can introduce significant error in the estimation of parameters of chemotaxis. In Dunn's chemotaxis chamber<sup>13</sup>, slowly changing gradients, with a half-life of decay estimated to be several hours, can be obtained after an initial dynamic stabilization period of about an hour. Although our device is more complex, it establishes the desired profile instantly and remains stable as long as flow is maintained (Fig. 1C, D). Because the technology described here generates stable linear gradients and provides the opportunity to observe and record migration in real time, an accurate and direct quantification

of the chemotaxis coefficient,  $\chi$ , is possible without prior knowledge of parameters such as the value of the random motility coefficient and its variation with the chemoattractant concentration<sup>25</sup> (Table 1).

The first step in IL-8-induced neutrophil chemotaxis is the ligation of the C-x-C receptors (IL-8RA and IL-8RB) on the cells<sup>30–32</sup>. Gradient steepness and mean agonist concentration are two of the most important parameters determining a neutrophil's ability to orient in a gradient<sup>20,33,34</sup>. The  $K_d$  for IL-8 receptors on isolated neutrophil membranes ranges from 5 to 12.4 nM<sup>35</sup>. We observed the maximal chemotaxis coefficient in a linear gradient with a maximum concentration of 6.3 nM (50 ng/ml), whereas the lowest gradient (0–0.63 nM) was entirely below the  $K_d$  range and  $\sim 80\%$  of the highest gradient (0–63 nM) was above the range. This receptor saturation at the highest gradient could directly cause the observed reduction in the chemotactic coefficient.

Our observations of neutrophil migration in gradients with complex shapes raise the possibility that these cells are far more adaptive to nonlinear environmental cues than has been thought previously. We report here that neutrophils can

detect a precipitous drop in concentration of IL-8, which they do not overshoot (Fig. 4B). A more gentle decrease in chemoattractant within the gradient results in the cells overshooting the locus of maximum IL-8 concentration (Fig. 4D). Taken together, the data from both types of gradients suggest a sensing mechanism in cells that has not been previously described. Alternatively, cell behavior in the “hill” gradient (Fig. 4D) may reflect a sluggish control mechanism within the cell. Notably, neutrophils have been shown to migrate down a local chemoattractant gradient in the presence of two competing chemoattractants<sup>24</sup>. Our results show that neutrophils can transiently migrate down the hill gradients even when only one chemoattractant is present. These data suggest that cells are responsive to local differences in chemoattractants.

Our data demonstrating that neutrophils are capable of complex migratory behavior raises the question of whether these results are physiologically relevant. Recent data demonstrate that soluble morphogen gradients are generated in developing embryos<sup>36,37</sup>. A careful study of bicoid deposition in *Drosophila* embryos demonstrated an exponential, anterior–posterior gradient of this morphogen<sup>38</sup>. In most instances, the concentration of chemoattractant is complicated by factors such as local degradation and/or endocytosis as well as sequestration within the extracellular matrix. Indeed, a recent paper demonstrated differences in the angiogenic activity of alternatively spliced forms of vascular endothelial growth factor (VEGF) depending on their location relative to the tumor source<sup>39</sup>. The more soluble isoforms promoted endothelial cell migration at a distance, whereas those that bound matrix were more effective closer to the tumor source. We speculate that chemoattractants are likely to adopt periodic shapes at sites of inflammation, given their differential synthesis

by point sources (cells) versus tissues (such as epithelium) and their selective degradation or retention by the extracellular matrix.

The microfluidic chemotaxis device and the assay described here provide an experimentally robust and highly adaptable method to study the behavior of chemotactic cells. In combination with other soft lithographic methods such as patterning cells, surfaces, and biomaterials, the microfluidic chemotaxis chamber will provide a basis for studying dynamic phenomena in cell biology or in tissue engineering applications. It should also facilitate massively parallel screening of candidate drugs that modulate chemotaxis.

### Experimental protocol

**Fabrication and characterization of chemotaxis device.** The microfluidic chemotaxis device was fabricated in PDMS using rapid prototyping and soft lithography<sup>19</sup>. The PDMS piece, with embedded microchannels and holes for the inlet and outlet ports, and a glass cover slip (25 mm × 50 mm) were treated in an oxygen plasma generator (150 mTorr, 100 W) for 1 min, after which they were placed against each other and irreversibly bonded. Polyethylene tubing with an outer diameter slightly larger than the inner diameter of the inlet port was inserted into the hole to make the fluidic connections. The pieces of tubing were then connected to a syringe pump containing medium and chemoattractant to complete the setup.

The cells were placed in the main channel immediately after the final recombination of the microchannels and allowed to migrate in a gradient of soluble chemical factors. Individual cells were followed using a tracking program (MetaMorph, Universal Imaging, Downingtown, PA). More than 95% of cells remained alive (Live/dead assay, Molecular Probes, Portland, OR) and motile during the entire period of experiment.

Device characterization was carried out using a fluorescent tracer, 10 kDa dextran-FITC (Sigma, St. Louis, MO). Fluorescent images were obtained at 5-min intervals from 0 to 60 min after the establishment of the gradient. Image analysis was carried out to obtain fluorescent intensities as a function of the width of the channel using Scion Image (Scion Corporation, Frederick, MD).

**Isolation of neutrophils.** Human whole blood was obtained from healthy volunteers by venipuncture into tubes containing sodium heparin (Becton Dickinson, San Jose, CA). Neutrophils were isolated by centrifugation of a tube containing 7 ml of whole blood layered over 4 ml of Mono-Poly Resolving Media (ICN, Irvine, CA) for 30 min at 2000 rpm (500g). The band of cells containing neutrophils was collected, washed several times, and resuspended in HBSS (Invitrogen, Carlsbad, CA) with 2 mg/ml of BSA (Sigma). Preparations contained >95% neutrophils, as assessed by staining with Wright's stain (Sigma).

**Preparation of chemoattractant.** Solutions of IL-8 (Sigma, concentrations: 5, 50, and 500 ng/ml) in HBSS were made and stored at -20°C until use.

**Time-lapse microscopy, image acquisition, and analysis.** Neutrophils were observed in a Zeiss Axiovert microscope (Zeiss, Thornwood, NY) through a 20× objective (Plan-Neofluar, Zeiss). Phase contrast images of neutrophils were taken every 20 s using a charge-coupled device camera (Hamamatsu, Hamamatsu, Japan). Image analysis was carried out using MetaMorph software.

### Acknowledgments

This study was partially supported by the Shriners Hospital for Children and the US National Institutes of Health (RR13322 and GM 56442).

### Competing interests statement

The authors declare that they have no competing financial interests.

Received 12 October 2001; accepted 11 April 2002

- Muller, A. *et al.* Involvement of chemokine receptors in breast cancer metastasis. *Nature* **410**, 50–56 (2001).
- Behar, T.N. *et al.* GABA-induced chemokinesis and NGF-induced chemotaxis of embryonic spinal cord neurons. *J. Neurosci.* **14**, 29–38 (1994).
- Wilkinson, P.C. *Chemotaxis and Inflammation* (Churchill Livingstone, New York, 1982).
- Yang, X.D., Corvalan, J.R., Wang, P., Roy, C.M. & Davis, C.G. Fully human anti-interleukin-8 monoclonal antibodies: potential therapeutics for the treatment of inflammatory disease states. *J. Leukoc. Biol.* **66**, 401–410 (1999).
- Clemons, M.J. *et al.* A randomized phase-II study of BB-10010 (macrophage inflammatory protein-1 $\alpha$ ) in patients with advanced breast cancer receiving 5-fluorouracil, adriamycin, and cyclophosphamide chemotherapy. *Blood* **92**, 1532–1540 (1998).
- Kolber, D.L., Knisely, T.L. & Maione, T.E. Inhibition of development of murine melanoma lung metastases by systemic administration of recombinant platelet factor 4. *J. Natl. Cancer Inst.* **87**, 304–309 (1995).
- Bignold, L.P. Measurement of chemotaxis of polymorphonuclear leukocytes *in vitro*. The problems of the control of gradients of chemotactic factors, of the control of the cells and of the separation of chemotaxis from chemokinesis. *J. Immunol. Methods* **108**, 1–18 (1988).
- Boyden, S.V. The chemotactic effect of mixtures of antibody and antigen on polymorphonuclear leukocytes. *J. Exp. Med.* **115**, 453 (1962).
- Brown, A.F. Neutrophil granulocytes: adhesion and locomotion on collagen substrata and in collagen matrices. *J. Cell Sci.* **58**, 455–467 (1982).
- Nelson, R.D., Quie, P.G. & Simmons, R.L. Chemotaxis under agarose: a new and simple method for measuring chemotaxis and spontaneous migration of human polymorphonuclear leukocytes and monocytes. *J. Immunol.* **115**, 1650–1656 (1975).
- Zigmond, S.H. Ability of polymorphonuclear leukocytes to orient in gradients of chemotactic factors. *J. Cell Biol.* **75**, 606–616 (1977).
- Adler, J. Chemoreceptors in bacteria: studies of chemotaxis reveal systems that detect attractants independently of their mechanisms. *Science* **166**, 1588–1597 (1969).
- Zicha, D., Dunn, G.A. & Brown, A.F. A new direct-viewing chemotaxis chamber. *J. Cell Sci.* **99**, 769–775 (1991).
- Dertinger, S.K., Chiu, D.T., Jeon, N.L. & Whitesides, G.M. Generation of gradients having complex shapes using microfluidic networks. *Anal. Chem.* **73**, 1240–1246 (2001).
- Chiu, D.T. *et al.* Patterned deposition of cells and proteins onto surfaces by using three-dimensional microfluidic systems. *Proc. Natl. Acad. Sci. USA* **97**, 2408–2413 (2000).
- Baggiolini, M., Dewald, B. & Moser, B. Human chemokines: an update. *Annu. Rev. Immunol.* **15**, 675–705 (1997).
- Campbell, J.J. & Butcher, E.C. Chemokines in tissue-specific and microenvironment-specific lymphocyte homing. *Curr. Opin. Immunol.* **12**, 336–341 (2000).
- Zlotnik, A. & Yoshie, O. Chemokines: a new classification system and their role in immunity. *Immunity* **12**, 121–127 (2000).
- Whitesides, G.M., Ostuni, E., Takayama, S., Jiang, X. & Ingeber, D.E. Soft lithography in biology and biochemistry. *Annu. Rev. Biomed. Eng.* **3**, 335–373 (2001).
- Haston, W.S. & Wilkinson, P.C. Locomotion and chemotaxis of leukocytes: gradient perception and locomotor capacity. *Curr. Opin. Immunol.* **1**, 5–9 (1989).
- Yoshimura, T., Matsuhiro, K., Oppenheim, J.J. & Leonard, E.J. Neutrophil chemotactic factor produced by lipopolysaccharide (LPS)-stimulated human blood mononuclear leukocytes: partial characterization and separation from interleukin 1 (IL 1). *J. Immunol.* **139**, 788–793 (1987).
- Yoshimura, T. *et al.* Purification of a human monocyte-derived neutrophil chemotactic factor that has peptide sequence similarity to other host defense cytokines. *Proc. Natl. Acad. Sci. USA* **84**, 9233–9237 (1987).
- Baggiolini, M., Dewald, B. & Moser, B. Interleukin-8 and related chemotactic cytokines—CXC and CC chemokines. *Adv. Immunol.* **55**, 97–179 (1994).
- Foxman, E.F., Campbell, J.J. & Butcher, E.C. Multistep navigation and the combinatorial control of leukocyte chemotaxis. *J. Cell Biol.* **139**, 1349–1360 (1997).
- Lauffenburger, D.A. & Linderman, J.J. *Receptors: Models for Binding, Trafficking, and Signaling* (Oxford Univ. Press, New York, 1993).
- Tranquillo, R.T., Zigmond, S.H. & Lauffenburger, D.A. Measurement of the chemotaxis coefficient for human neutrophils in the under-agarose migration assay. *Cell Motil. Cytoskeleton* **11**, 1–15 (1988).
- Ismagilov, R.F., Stroock, A.D., Kenis, P.J.A., Whitesides, G. & Stone, H.A. Experimental and theoretical scaling laws for transverse diffusive broadening in two-phase laminar flows in microchannels. *Appl. Phys. Lett.* **76**, 2376–2378 (2000).
- Moghe, P.V., Nelson, R.D. & Tranquillo, R.T. Cytokine-stimulated chemotaxis of human neutrophils in a 3-D conjoined fibrin gel assay. *J. Immunol. Methods* **180**, 193–211 (1995).
- Lauffenburger, D.A. & Zigmond, S.H. Chemotactic factor concentration gradients in chemotaxis assay systems. *J. Immunol. Methods* **40**, 45–60 (1981).
- Firtel, R.A. & Chung, C.Y. The molecular genetics of chemotaxis: sensing and responding to chemoattractant gradients. *Bioessays* **22**, 603–615 (2000).
- Parent, C.A. & Devreotes, P.N. A cell's sense of direction. *Science* **284**, 765–770 (1999).
- Murphy, P.M. & Tiffany, H.L. Cloning of complementary DNA encoding a functional human interleukin-8 receptor. *Science* **253**, 1280–1283 (1991).
- Devreotes, P.N. & Zigmond, S.H. Chemotaxis in eukaryotic cells: a focus on leukocytes and *Dictyostellium*. *Annu. Rev. Cell Biol.* **4**, 649–686 (1988).
- Zigmond, S.H. Ability of PMN leukocytes to orient in gradients of chemotactic factors. *J. Cell Biol.* **75**, 606–616 (1977).
- Barnett, M.L., Lamb, K.A., Costello, K.M. & Pike, M.C. Characterization of interleukin-8 receptors in human neutrophil membranes: regulation by guanine nucleotides. *Biochim. Biophys. Acta* **1177**, 275–282 (1993).
- Strigini, M. & Cohen, S.M. Wingless gradient formation in the *Drosophila* wing. *Curr. Biol.* **10**, 293–300 (2000).
- McDowell, N., Gurdon, J.B. & Grainger, D.J. Formation of a functional morphogen gradient by a passive process in tissue from the early *Xenopus* embryo. *Int. J. Dev. Biol.* **45**, 199–207 (2001).
- Driever, W. & Nusslein-Volhard, C. The bicoid protein determines position in the *Drosophila* embryo in a concentration-dependent manner. *Cell* **54**, 95–104 (1988).
- Grunstein, J., Masbad, J.J., Hickey, R., Giordano, F. & Johnson, R.S. Isoforms of vascular endothelial growth factor act in a coordinate fashion to recruit and expand tumor vasculature. *Mol. Cell Biol.* **20**, 7282–7291 (2000).